XI International Conference on Computational Plasticity. Fundamentals and Applications
COMPLAS XI
E. Oñate, D.R.J. Owen, D. Peric and B. Suárez (Eds)

THE CONTACT TEMPERATURE AND DEFORMATION AREA OF ASPERITIES ON ROUGH SURFACE FOR THREE- BODY CONTACT SITUATION

Jeng-Haur Horng *, Chin-Chung Wei *, Yang-Yuan Chen † and Shin-Yuh Chern*

* Department of Power Mechanical Engineering,
National Formosa University, Yunlin, Taiwan
e-mail: jhhorng@gmail.com, ccwei@nfu.edu.tw, kevindga@nfu.edu.tw

† Department of Systems and Naval Mechatronic Engineering,
National Cheng Kung University, Tainan, Taiwan
Email: td7211@gmail.com

Key words: Micro-Machine, Contact Temperature, Three-Body Microcontact, Friction Coefficient, Plasticity Index.

Abstract. In the micro-machine or precision machine, particles are often presented at contact interfaces. And these particles will affect the variation of plastic deformation of asperities and the contact temperature between the contact surfaces. In this paper, we used three-body microcontact model and contact temperature theory to evaluate elastic contact area, plastic contact area, elastic-plastically deformed contact area and contact temperature under the different particle sizes, velocities and applied loads conditions. The friction force is one of the main heat resources of contact temperature. Because friction coefficient is variable parameter in this work, the contact temperature rise between the contact surfaces is larger than that of assuming the constant friction coefficient conditions of CrMo steel for the different loads. The contact temperatures of particles and asperity increase when the velocity and applied load increase. The increases of particle size will give rise to the increase of particle temperature and decrease of asperity temperature on rough surface. The plastic deformed contact area increases when the particle size and particle density increase.

1 INTRODUCTION

When the precision machine or the micro machine operate and the two surfaces make contact, will cause the asperity and particles has the elastic, elasto-plastic, or plastic contact deformation between surface roughness. The practical contact area is the sum of the areas of the contact surface summits and only a small part of the vision area [1, 2]. The most widely used stochastic model to predict the real contact area is that proposed by Greenwood and Williamson (GWmodel) [3]. The experimental observations of Pullen and Williamson (PW model) [4] showed that, in the plastic deformation state, volume is conserved by a rise in the non-contacting surface under extremely high loading. Chang et al. [5] proposed an elastic–plastic microcontact model (CEB model) to study the contact properties of rough surfaces. Research using this model has shown that the GW model of fully elastic surface microgeometry and the PW model of fully plastic surface microgeometry have two limiting cases of the general elastic–plastic contact. Horng [6] proposed a generalized elliptic elastic–plastic microcontact model (H model) that takes into account the directional nature of surface roughness for elliptic contact spots between anisotropic rough surfaces. This model can be simplified to become the GW, PW, on CEB model. Kogut and Etsion [7] (KE model) presented elastic–plastic asperity models to modify the shortcomings of the transition from elastic deformation to fully plastic deformation in other models.

When two bodies slide relative to each other, the friction heat is expened at a restuiced number of contact spots between two surfaces or surface and particle. The maximum local temperature generated at the contact spot, called the flash temperature, is higher than that at the surrounding area. The flash temperature is one of the reasons causing fatigue, high wear and failure of material. It produced at rubbing contact are of shot duration (say 10^{-3}s or less) and occur only over small dimensions (say10^{-4}m or less). They are therefore difficult to measure and, in the interpretation of almost all experiments, recourse is generally made to estimating their magnitude using the theory originally formulated by Blok [8] and Jaeger [9]. Geeim and Winer [10] considered the transient temperature rise in the vicinity of a microcontact. Tian and Kennedy [11] used the green function method to obtain Peclet numbers of the approximation of flash temperatures. Compared to isolated contact, there are selective few contributions in the literature on flash temperature in multiple contact conditions. Ling [12] develops a method for studying two comparably rough surfaces and generating the statistics of their interaction. Results show that, with time, the interaction between contacts mitigates the effects of velocity somewhat. Knothe and Liebelt [13] studied contact temperature and temperature fields of components by Laplace transforms and the Green's functions. The results show that different kind of topography causes different rise of the maximum contact temperature for wheel-rail system. Up to now, very few work discuss the contact temperature for three-body contact situations. This work study a more generalized three-body contact temperature model and discusses the effect of each operating parameter on contact temperatures.

2 ANALYSIS

2.1 Microcontact model

In the contact model, we made the following assumptions: 1. All surface asperities are far

apart and there is no interaction between them. 2. There is no bulk deformation, only the surface asperities deform during contact. 3. The diameter of spherical particles is D and much harder than the upper and lower contact surfaces, which deform plastically during contact with particles. 4. Slopes of surface asperities are negligibly small. Figure 1 shows the geometry of the three contacting bodies : surface 1, surface 2, and the particles. Here, z and d denote the asperity height and separation of surfaces, respectively.

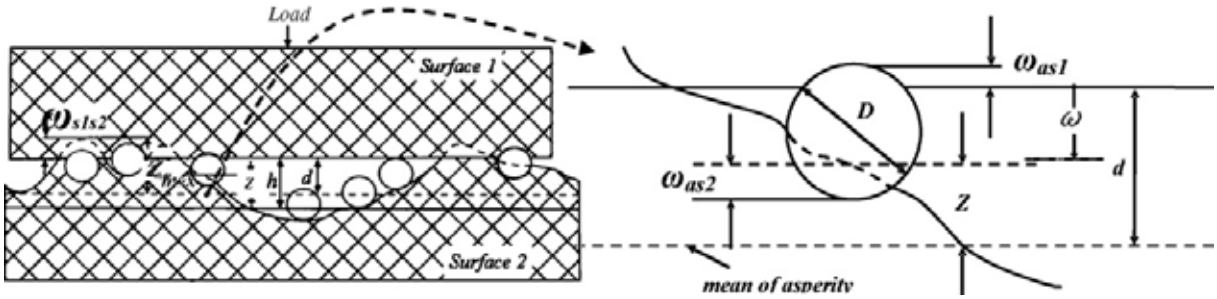

Figure 1: Geometry of three contacting bodies

According to the paper [2], the tree-body microcontact model becomes:

$$F_{total} = F_{as1} + F_{s1s2-as1} = \frac{\pi H_{s1} H_{s2} \eta_a A_n}{H_{s1} + H_{s2}} \left[\frac{9\pi^2}{4} \left(\frac{H_{s1}^2}{E_{as1}^2} + \frac{H_{s2}^2}{E_{s1s2}^2} \right) \int_{d-h_e}^{d} x^2 \phi_a(x) dx + \int_{d}^{x_{max}} x^2 \phi_a(x) dx \right] + \left(1 - \frac{\pi H_{s1} \eta_a}{H_{s1} + H_{s2}} \int_{X_{min}}^{X_{max}} x^2 \phi_a(x) dx \right) \cdot F_{s1s2} \quad (1)$$

$$A_{total} = A_{as1} + A_{s1s2-as1} = \frac{\pi H_{s2} \eta_a A_n}{H_{s2} + H_{s1}} \left[\frac{9\pi^2}{4} \left(\frac{H_{s1}^2}{E_{as1}^2} + \frac{H_{s2}^2}{E_{s1s2}^2} \right) \int_{d-h_e}^{d} x^2 \phi_a(x) dx + \int_{d}^{X\max} x^2 \phi_a(x) dx + A_{s1s2} \right] \cdot \left\{ 1 - \frac{\pi H_{s1} \eta_a}{H_{s1} + H_{s2}} \int_{d}^{X_{max}} x^2 \phi_a(x) dx \right\} \quad (2)$$

where A_{s1s2} is the real total contact area of the two-body microcontact models. The total contact areas A_t, and the total contact load F_t of the three bodies can be obtained from Eq. (1) and (2).

2.2 Friction model

Our friction analysis model is based on the analyses of Komvopoulos et al. [14] and Bhushan et al.[15-16]. The friction is expressed as the sum of four components: surface asperity deformation (μ_d), plowing deformation by particles entrapped between contact surface (μ_a), adhesive friction (μ_s), and ratchet friction (μ_r) at the contact region. The total friction force and friction components become:

$$\mu = \mu_d + \mu_a + \mu_s + \mu_r = A_r \tau_a + A_{s1s2\text{-}s1a} \tau_{s1s2} + A_{s1a} \tau_{s1a} + A_{s1s2\text{-}s1a} \tau_{s1s2} \times tan^2\theta \quad (3)$$

where A_r, $A_{s1s2\text{-}s1a}$, and A_{s1a} are the real areas of contact during adhesion, two surface

deformation, and particle-surface 1 deformation, respectively. They are calculated from Eq(1). τ_a, τ_{s1s2}, and τ_{s1a}, are the shear strengths during adhesion, two surface deformation, and particle-surface deformation [16],respectively.

2.3 Flash temperature model

Frictions were made when the surface 1, surface 2, and particles made contact, and the energy consumed was mostly converted to heat. This caused an increase in surface temperature, and heat generated was determined using the following equation,

$$Q=\mu FV \tag{4}$$

Where μ is the friction coefficient, V is the relative speed, and F is the normal load. The heat conductance quantity of a unit area was used to express the magnitude heat conductance.

$$q=\frac{Q}{A}=\frac{\mu FV}{\pi a^2}=\mu P_m V \tag{5}$$

A is the practical contact area and a is the contact radius.

The Peclet Number (P_e) is a nondimensional speed parameter used to evaluate the movement rate of contact heat. It is defined as：

$$P_e=\frac{Va}{2\alpha}=\frac{Va\rho C}{2K} \tag{6}$$

Where a is contact heat, α is the rate of heat diffusion ($\alpha=K/\rho C$), K is the heat conductance coefficient, ρ is the density, and C is the specific heat. Different Peclet Numbers exist at different velocities. Tian and Kennedy [8] proposed a model whose maximum temperature could be applied to all Peclet Numbers. The average temperature increase of its spherical contact heat as expressed as

$$T=\frac{1.22qa}{K\sqrt{\pi(0.6575+P_e)}} \tag{7}$$

When $F_{ai}=F_{as1,max}$, the maximum temperature when the abrasive particles made contact with the workpiece is

$$T_{as1,\max}=\frac{1.22\mu_a V\sqrt{F_{as1,\max}H_{s1}}}{\pi\left[K_{s1}\sqrt{(0.6575+P_{e,s1})}+K_a\sqrt{(0.6575+P_{e,a})}\right]} \tag{8}$$

Therefore, the increase of relative velocity will result in the increase of contact temperature. and the average temperature between the abrasive particle and workpiece is

$$T_{as1,ave}=\frac{\int_{x_{\min}}^{x_{\max}}T_{as1}\phi_a(x)dx}{\int_{x_{\min}}^{x_{\max}}\phi_a(x)dx} \tag{9}$$

3 RESULTS AND DISCUSSION

This paper study three-body contact temperature for the different particle sizes, particle densities and the relative velocities. The maximum contact temperature, average contact temperature and deformation area between particle and asperity were calculated. The material used in the analysis was CrMo steel.

Fig.2 (a) shows the maximum contact temperature $T_{as1,max}$, average contact temperature $T_{as1,ave}$, and total friction coefficient μ_{total} versus applied loads. It is interesting to note that the maximum contact temperature and average contact temperature increased linearly with increasing applied loads. The maximum contact temperature was higher than the average contact temperature for the different loads. Fig.2 (b) shows the surface and particle friction coefficients versus applied loads for the different particle size when Ψ = 1.5, Rq = 100 nm, and v = 0.2 m/s. The total friction coefficient is the sum of surface friction coefficient and particle friction coefficient. When particle size is 500 nm, and the intersection pressure of the particle and the surface friction coefficient is about 2 MPa; but when the particle size decreases to 300nm and 100nm, the intersection pressure of the particle and the surface friction coefficient increase to 5 MPa and 50 MPa. The bigger the size of particle, the larger the total friction coefficient. Fig.2 (c) shows the elastic, elastic-plastic and plastic deformed

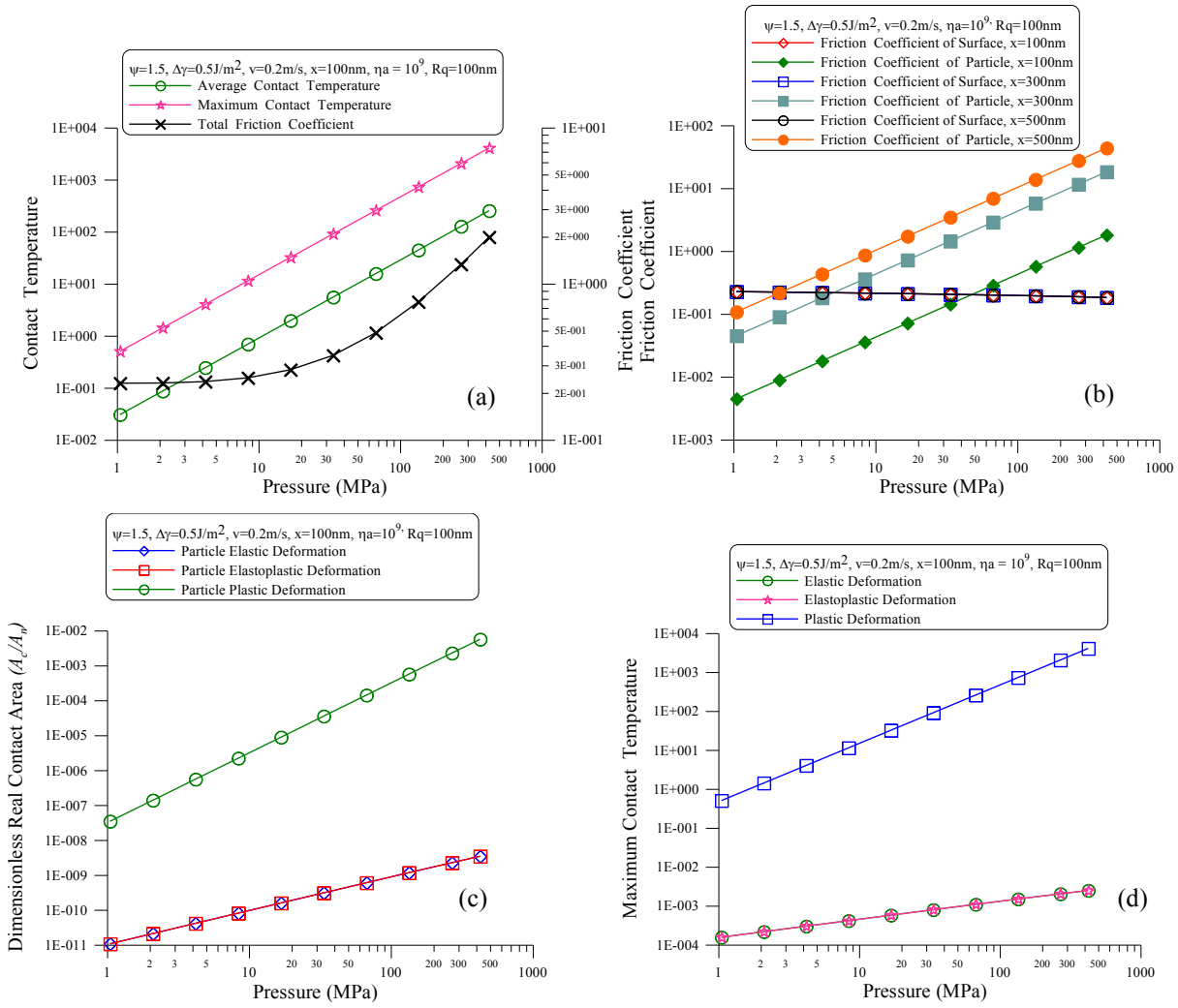

Figure 2: (a) Contact temperature and total friction coefficient varying with applied loads;(b) The surface and particle friction coefficients varying with applied loads when different particle size;(c) The dimensionless real contact area components varying with applied loads; (d) The maximum contact temperature components varying with applied loads

real contact area of particles. the real contact area increased with increasing applied loads. The plastic deformed real contact area is larger than the elastic and elastic-plastic deformed real contact area. Results indicate that the real deformation contact area of particle is mainly affected by the plastic deformation. Fig.2 (d) shows three kinds of maximum contact temperature of particles for the different deformed areas. The maximum contact temperature of plastic deforming controls the maximum contact temperature. The trend of the maximum contact temperature is the similar with the deformation area in Fig.2 (c). It indicates that the particle plastic deformation area has a significant effect on the maximum contact temperature between two sliding surfaces.

Fig.3 (a) and Fig.3 (b) are the different relative velocity's relationship with average and maximum contact temperature for the particle density $\eta_a=10^9 m^{-2}$, surface roughness Rq=100nm, relative velocity v=0.2 m/s. The average contact temperature and the maximum contact temperature increase with increasing pressure and particle size. Because the increase of particle size will result in the increase of particle load and then increase the contact temperature of particle. It indicates that effectively control of the particle size between the contact interface of mechanical elements can reduce the contact temperature.

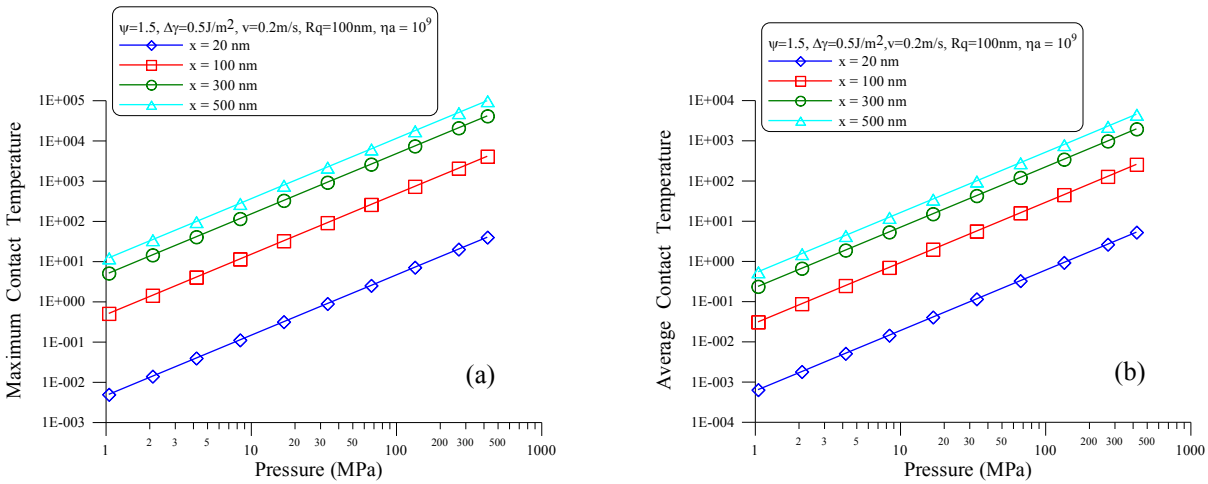

Figure 3: Relationship between particle contact temperature and applied loads of different particles size

Fig.4 (a) and Fig.4 (b) are the different relative velocity's relationship with average and maximum contact temperature for the particle size x=100nm, surface roughness Rq=100nm, relative velocity v=0.2 m/s. The average contact temperature and the maximum contact temperature increase with increasing pressure. Because the increase of particle density will result in the increase of particle load and then increase the contact temperature of particle. It indicates that decrease the wear debris between the contact interface of mechanical elements can reduce the contact temperature.

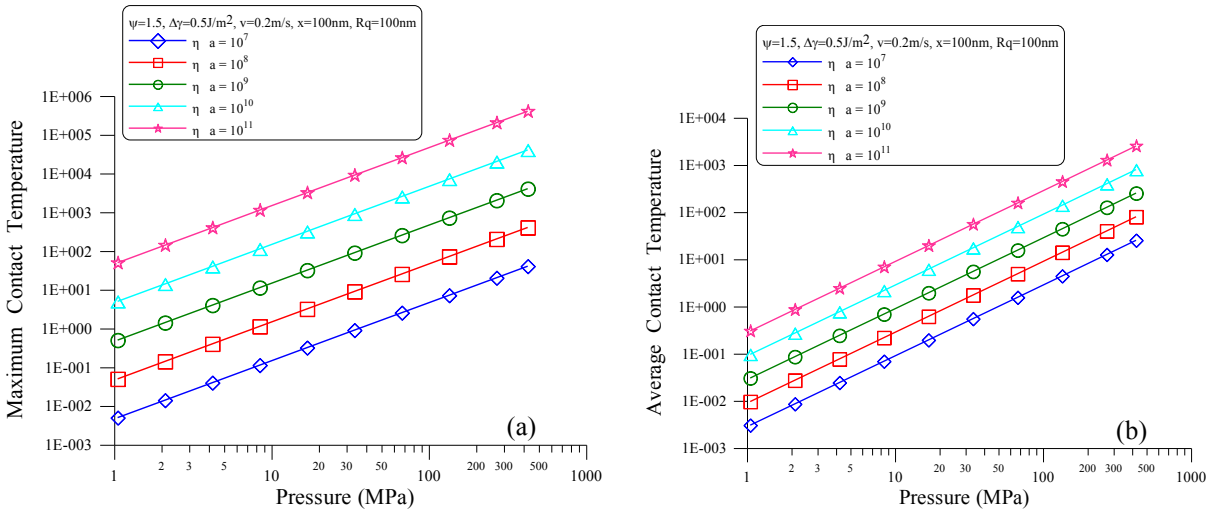

Figure 4: Relationship between particle contact temperature and applied loads of different particles density

4 CONCLUSIONS

- The trend of the maximum contact temperature of two surfaces is the similar with the particle plastic deformation area. It indicates that the particle plastic deformation area has a significant effect on the maximum contact temperature between two sliding surfaces.
- In contact interface, the contact temperatures of particles and asperity increase when the velocity and applied load increase
- The increase of particle size and density will result in the increase of particle load for three-body contact condition. It indicates that decrease the particle size or wear debris between the contact interface of mechanical elements can reduce the contact temperature.

REFERENCES

[1] Kikuchi, N. and Oden, J. T. *Contact problems in elasticity.* SIAM, in Press, (1988).

[2] Horng, J. H. and Wei C. C. A study of surface friction and particle friction between rough surfaces. *Wear* (2009) **267**:1257-1263.

[3] Greenwood, J. A. and Williamson, J. B. P. Contact of nominal flat surface. *Proc. R. Soc. London, Ser. A.*(1996) **295**:300-319.

[4] Pullen, J. and Williamson, J. B. P. On the plastic contact of rough surface.*Proc. R. Soc. London* (1972) **327**:157-173.

[5] Chang, W. R., Etsion, I. and Bogy, D. B. An elastic-plastic model for the contact of rough Surface. *ASME Journal of Tribology* (1987) **110**:50-56.

[6] Homg, J. H. An elliptic elastic-plastic asperity microcontact model for rough surface. *ASME Journal of Tribology* (1988) **120**:82-88.

[7] Kogut, L. and Etsion, I. Elastic-plastic contact analysis of a sphere and a rigid flat. *ASME Journal of Applied Mechanics* (2002) **69**:657-662.

[8] Blok, H. Theoretical study of temperature rise at surfaces of actual contact under oiliness lubricating conditions. General discussion on lubrication, *Proc. Inst. Mech. Eng.*

London (1937) **2**: 222-235.

[9] Jaeger, J. C. Moving sources of heat and the temperature at sliding surfaces. *Proc. R.Soc. NSW* (1942) **66**: 203-224.

[10] Geeim, B. and Winer, W. O. Transient temperatures in the vicinity of asperity contact. *ASME J. Tribology* (1985) **107**: 333-342.

[11] Tian, X., and Kennedy, F.E., " Maximum and Average Flash Temperatures in Sliding Contacts, " ASME journal of Tribology (1994) **116 NO.1**:167-174.

[12] Ling, F. F. On temperature transients at sliding interface. *ASME J. Lubrication Technology* (1969) **91** : 397-405.

[13] Knothe, K. and Liebelt, S. Determination of temperatures for sliding contact with applications for wheel-rail system. *Wear* (1995) **189** : 91-99.

[14] Komvopoulos, K., Saka, N. and Suh, N. P. Plowing friction in dry and lubricated metal sliding. *ASME Journal of Tribology* (1986) **108**:301-313.

[15] Bhushan, B. and Nosonovsky, M. Scale effects in friction using strain gradient plasticity and dislocation-assisted sliding (microslip). *Acta Mater* (2003) **51**:4331–4345.

[16] Bhushan, B. and Nosonovsky, M. Comprehensive model for scale effects in friction due to adhesion and two- and three-body deformation (plowing). *Acta Mater* (2004) **52**:2461-2474.

[17] Chen, W. W. and Wang, Q. Thermo-mechanical analysis of elasto-plastic bodies in a sliding spherical contact and the effect of sliding speed, heat partition, and thermal softening. *ASME J. Tribology* (2008) **130**:041402-1~041402-10.

[18] Horng, J. H., Lee, J. S., Ku, M. Y. and Chen, C. H. Fractal contact model between rough surfaces in considering elastoplastic deformation and adhesion force. *Key Engineering Material, March* (2008) **364~366**:442~448.